

Two-step dopant diffusion study performed in two dimensions by scanning capacitance microscopy and TSUPREM IV

J. Kim, J. S. McMurray, and C. C. Williams^{a)}

Department of Physics, University of Utah, Salt Lake City, Utah 84112

J. Slinkman

IBM Microelectronics, Essex Junction, Vermont 05452

(Received 12 February 1998; accepted for publication 30 April 1998)

We report the results of a two-step two-dimensional (2D) diffusion study by scanning capacitance microscopy (SCM) and 2D SUPREM IV process simulation. A quantitative 2D dopant profile of a gate-like structure is measured with the SCM on a cross-sectioned polished silicon wafer. The gate-like structures consist of heavily implanted n^+ regions separated by a lighter doped n -type region underneath $0.56 \mu\text{m}$ gates. The SCM is operated in the constant-change-in-capacitance mode. The 2D SCM data are converted to dopant density through a physical model of the SCM/silicon interaction. This profile has been directly compared with 2D SUPREM IV process simulation and used to calibrate the simulation parameters. The sample is then further subjected to an additional diffusion in a furnace for 80 min at 1000°C . The SCM measurement is repeated on the diffused sample. This final 2D dopant profile is compared with a SUPREM IV process simulation tuned to fit the earlier profile with no change in the parameters except the temperature and time for the additional diffusion. Our results indicate that there is still a significant disagreement between the two profiles in the lateral direction. SUPREM IV simulation considerably underestimates the diffusion under the gate region. © 1998 American Institute of Physics. [S0021-8979(98)05715-6]

I. INTRODUCTION

Quantitative two-dimensional (2D) dopant profiling is very important for the calibration of process simulators, which is identified in the National Technology Roadmap for Semiconductors as one of the significant needs of the semiconductor industry.¹ Several techniques are currently under development which show promise for high resolution 2D dopant profiling. These include dopant sensitive chemical etch techniques, nano-SRP and SCM. These techniques have been recently reviewed by Diebold *et al.*² The scanning capacitance microscope (SCM) has been shown to be capable of quantitative 2D profiling.³⁻⁶ In a previous study, quantitative 2D dopant profiling of a gate-like structure was obtained using SCM.⁷ Furthermore, we have made a direct comparison of the SCM results with the predictions of a technology computer-aided design (TCAD) process simulator TSUPREM4.⁸ In this work, we performed a two-step diffusion experiment and address the plausibility of calibrating the process simulator with the SCM measurements.

II. EXPERIMENTS

In the SCM technique, an atomic force microscope (AFM) is used to position a conducting tip at a semiconductor surface, and local capacitance is measured with the aid of a sensitive capacitance sensor electrically connected to the tip. As the tip is scanned, both topographic and capacitance data are acquired simultaneously. For the measurements dis-

cussed, a NanoScope IIIa AFM/SCM, with a Dimension 3000 head manufactured by Digital Instruments, is used. Some of the measurements were performed with an RCA capacitance sensor.⁹ This sensor uses a 915 MHz probing voltage for capacitance detection. In this configuration, the input capacitance to the RCA sensor is about 1 pF. Since most of this is stray capacitance, it is necessary to look for changes in capacitance to separate the small tip capacitance from the much larger stray capacitance. This is accomplished by applying a time varying bias voltage to the semiconducting sample. The bias voltage typically has a frequency between 5 and 15 kHz. This bias voltage modulates the depletion capacitance in the semiconductor. This SCM configuration has been successfully used with both commercial and home-built AFMs.^{10,11}

While it is straightforward to measure the change in capacitance at each point with a lock-in amplifier, resolution degradation may occur in lightly doped areas since the resolution of the SCM is determined by the volume of silicon that is depleted. To overcome this problem, the SCM is operated in a constant-change-in-capacitance mode, where the change in capacitance measured by the sensor is small and is held constant by varying the amplitude of the bias applied to the sample with a feedback control.³ This leads to large bias voltages in heavily doped regions where the depletion is small due to the large number of carriers and a small bias in lightly doped regions. Using this configuration, the SCM resolution is limited by the diameter of the tip.

The 2D profile reported here is obtained on an n -type sample (IBM XG33 sample, sample 1) that is implanted with

^{a)}Electronic mail: clayton@physics.utah.edu

phosphorus atoms. The substrate doping level is approximately 10^{15} cm^{-3} and the peak concentration is $8 \times 10^{19} \text{ cm}^{-3}$, as measured by secondary ion mass spectroscopy (SIMS). The area of interest is a series of gate-like structures, heavily implanted regions separated by a lighter doped region underneath the gates. These structures are created by ion implantation, with $0.56\text{-}\mu\text{m}$ -wide lines of oxide to mask the gate area. For the diffusion experiment, a piece of the wafer has been annealed in a nitrogen ambient furnace for 80 min at 1000°C (sample 2). The samples are then cleaved and polished to the desired implanted area. The polishing is performed using a series of diamond embedded polishing pads. It is found that having a scratch-free surface is very important in order to avoid the modification of the capacitance signal by the topographic features. The smallest diamond particle size was $0.1 \mu\text{m}$. At the final polishing step, a colloidal silica solution is used. Beside providing the final polish for the surface, this step also provides surface insulation and passivation. The C - V curves generated with the SCM indicate that the insulating layer on the surface after polishing is thin (about 3 nm) and of sufficient quality to be useful for SCM. We find that it is sometimes necessary to anneal the sample at $\sim 200^\circ\text{C}$ to drive excess moisture off the surface. This additional annealing also seems to improve the quality of the insulating layer. A detailed study of sample preparation will be published separately.

Operating the SCM in the constant-change-in-capacitance mode requires slow scan rates. The data collected has 512 points per line and 128 lines per image. The 128 lines are interpolated to 512 lines. The data is processed with a sixteen pixel Gaussian filter in both the x and y directions before the conversion to reduce noise. The Gaussian width used in the filter has an effective width smaller than the tip's radius. The tips used in this study have a radius of $\sim 30 \text{ nm}$. The data is also corrected for a lateral drift due to thermal expansion and piezo creep. Drift rate can be measured by comparing the positions of a particular feature on two separate images. The effects of drift were corrected with post processing software. The spatial error in the image after correction is estimated to be less than 5 nm.

The amplitude of the bias voltage measured in the constant change in capacitance mode is related to the dopant density through a conversion algorithm. The algorithm is based on a quasi-3D model of the tip sample capacitor.⁴ Using this method, high resolution vertical dopant profiles on silicon wafers have been achieved.³⁻⁵ These profiles are found to be in good agreement with vertical SIMS measurements.

The conversion algorithm requires several parameters: tip radius, peak dopant density and corresponding ac bias, oxide thickness, oxide dielectric constant, and size of the SCM sensor probing voltage. In this measurement a heavily doped silicon tip with a radius of 37 nm (determined by imaging a Niobium film)¹² was used. The reference dopant value used in this conversion is $8 \times 10^{19} \text{ atoms cm}^{-3}$, as determined by SIMS. Changing any of the other model parameters (oxide thickness, dielectric constant, or the amplitude of the sensor probing voltage) have a similar effect; they all affect the lowest dopant value generated with the conversion

process. Currently none of these parameters are exactly known, but reasonable values can be chosen for two of the three, and the third varied as a free parameter within reasonable limits. The two values fixed in this conversion are the oxide thickness and the oxide dielectric constant. The thickness is chosen to be 3 nm, slightly larger than a native silicon oxide. The value of the dielectric constant used is 3.0. The value of the free parameter, the sensor probing voltage, is adjusted so that the dopant profile taken in the vertical direction in an implanted region most closely fits the SIMS profile. In this case, the probing voltages used were 1.15 V peak for sample 1, and 1.7 V peak for sample 2.

In our earlier report,⁷ we have shown that the percentage difference of SCM and SIMS in the vertical profile is 15%, and the accuracy in the full 2D image should be comparable to that of the vertical profile.

We used the commercially available process simulator, TSUPREM4¹³ for the prediction of the 2D dopant profiles, which can be cross checked against SIMS in the 1D vertical direction.

The full fabrication process of the XG33 sample was simulated with TSUPREM4.⁸ We used "out-of-the-box" default model parameters for phosphorus diffusion with a minor adjustment to the best fit to the SIMS of the phosphorus dopant in the unmasked region of sample originally annealed in the oxidizing ambient at 900°C .

III. RESULTS AND DISCUSSION

Figure 1(a) shows a comparison of vertical profiles from SCM, SIMS, and TSUPREM4 simulation using out-of-the-box parameters obtained on the as-processed XG33 sample (sample 1). While the SIMS and SCM results show excellent agreement, TSUPREM4 process simulation underestimates the dopant concentrations between 0.1 and $0.4 \mu\text{m}$ (8×10^{19} to $1 \times 10^{18} \text{ cm}^{-3}$). Full 2D comparison of SCM and TSUPREM4 is shown in Fig. 1(b) as contour plots for sample 1. The position of the gate corresponds to the bottom center of the figure. The lateral diffusion underneath the gate is underestimated by the TCAD simulation. This is further illustrated in Fig. 1(c), which is a lateral line cut taken at a depth of $0.1 \mu\text{m}$. In contrast, the $1 \times 10^{17} \text{ cm}^{-3}$ level of the simulation is too deep in the vertical direction far from the gate, but the SCM and TSUPREM4 contours at this low concentration is in moderate agreement below the gate [see Fig. 1(a)].

We have attempted further tuning of the TSUPREM4 process simulator to fit the full 2D SCM results by adjusting a few physically significant parameters. One of the results is shown in the contour plot of Fig. 2. For this comparison, a few adjustments in the parameters have been made for better fit in both vertical and lateral direction. To achieve the improved fit, the bulk interstitial recombination rate was increased by $10\times$ and the surface interstitial recombination velocity was decreased by $0.1\times$. These adjustments improved the fit significantly, as seen in Fig. 2. While there are still some discrepancies close to the gate region, overall fit is much better than that shown in Fig. 1(b). With the simulator tuned both laterally as well as vertically, we now turn to the

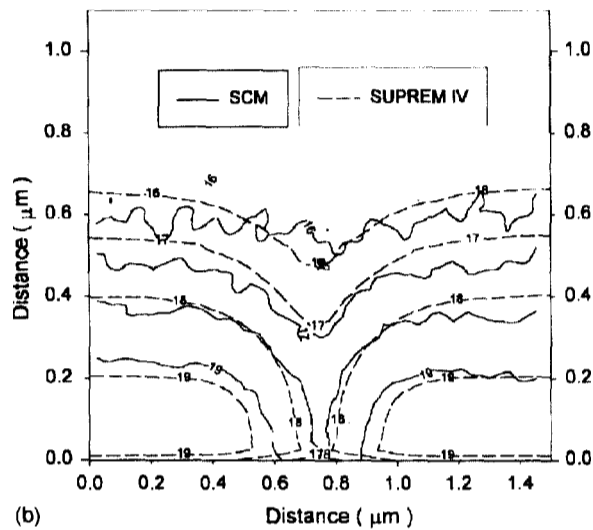
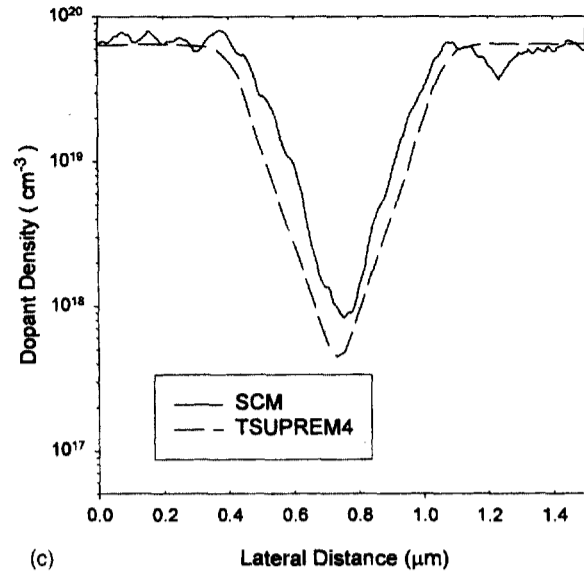
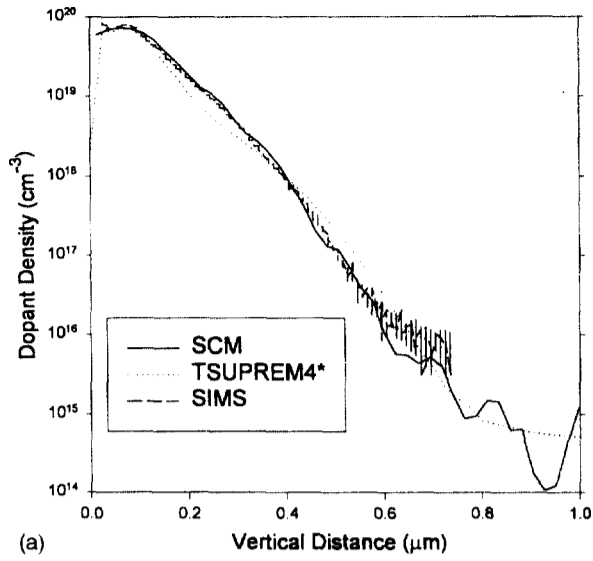


FIG. 1. (a) Vertical profiles of original XG33 sample (sample 1). TS4 simulation underestimates the dopant concentration between 0.1 μm and 0.4 μm . (b) Comparison of SCM results on the original XG33 sample with TSUPREM4 simulation with out-of-the-box parameters. Numbers on the contour lines represent dopant concentration in $\log[\text{density}(\text{cm}^{-3})]$. (c) Lateral profile under the gate region for the original XG33 sample. Note the discrepancy between the SCM and TSUPREM4 results.

measurements on sample 2, which has been subjected to an additional diffusion in a furnace for 80 min at 1000 °C. A vertical SIMS profile has been performed for this sample far from the masked region and used for cross comparison. For the TSUPREM4 simulation, the parameters that provided best fit (vertically and laterally) for the original sample (sample 1) have been used, only the additional diffusion time and temperature has been changed. For the conversion, peak concentration taken from the TSUPREM4 simulation and the lowest concentration have been used as pinning concentrations, while the other parameters remain the same. For the 2D SCM profiles no further optimization to SIMS profiles was used. Figure 3 shows the vertical profile of the diffused sample (sample 2) away from the gate. It can be seen that SCM, TS4, and SIMS agree moderately in the vertical direction down to $1 \times 10^{17} \text{ cm}^{-3}$. The TS4 simulation results have an excellent agreement with the SCM profile in the vertical direction.

A full 2D comparison of SCM and TS4 simulation is shown in Fig. 4. As can be readily seen, the contour lines agree relatively well over most of the image. However, near

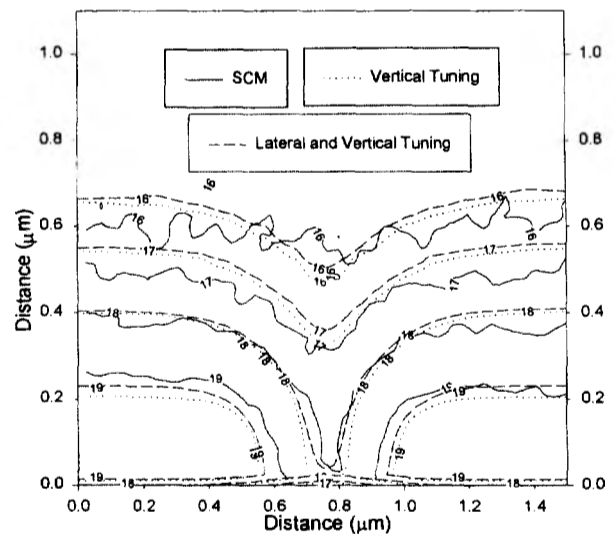


FIG. 2. Comparison of TSUPREM4 simulation and SCM dopant profiles for the original XG33 sample (sample 1). For better lateral fit, surface interstitial recombination velocity has been adjusted to $0.1\times$ and bulk interstitial recombination rate to $10\times$ to TS4 default parameters. Numbers on the contour lines represent dopant concentration in $\log[\text{density}(\text{cm}^{-3})]$.

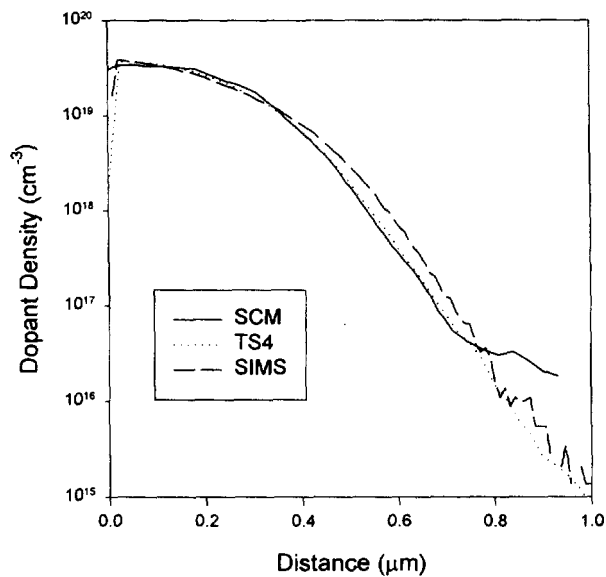


FIG. 3. Vertical dopant profile of XG33 sample after an additional 80 min anneal (sample 2) at 1000 °C in the inert ambient.

and under the gate region, we can still see quite a good deal of disagreement between the two profiles. This is illustrated in Fig. 4(b) where lateral cuts 0.1 and 0.4 μm under the surface is plotted. While the two show excellent agreement at 0.4 μm , the TS4 result significantly underestimates the diffusion at 0.1 μm under the gate.

In addition to phosphorus diffusion coefficients for both interstitial- and vacancy-mediated diffusion species, TSUPREM4 also accounts for the diffusion and recombination of the interstitial and point defects themselves. The recombination and generation of point defects at the silicon surface and in the bulk are also accounted for. Specifically, when oxidation occurs, such as for the initially annealed XG33 sample (sample 1), the latter kinetics are dominant, since oxidation is known to inject interstitials into the silicon bulk from the surface. As a result, the interstitial concentration is far in excess of equilibrium during oxidation. During the final 80 min anneal in the inert ambient, the point defect will have relaxed to equilibrium. The TSUPREM4 coefficients for surface and bulk point-defect generation and recombination were tuned to fit the 900 °C oxidation SIMS data. For the simulation of the subsequent 80 min inert anneal it may well be the case that the point-defect generation model parameters are not accurate, causing TSUPREM4 to underestimate the lateral outdiffusion. It is most likely that the surface generation/recombination rate is incorrect, since the simulated, SIMS, and SCM vertical profiles at 80 min still match fairly well.

We also note that in actual practice, i.e., in the modeling of production level devices, which can require the modeling of upwards of order one hundred annealing steps (including furnace ramps), 2D simulations of actual metal-oxide-semiconductor-field-effect transistor (MOSFET) source-drain junctions more often than not underpredict the lateral outdiffusion for inert junction anneals. It is more the case for boron (ip^+) source-drains, but it is also observed for phosphorus (n^+). Our result is consistent with the general

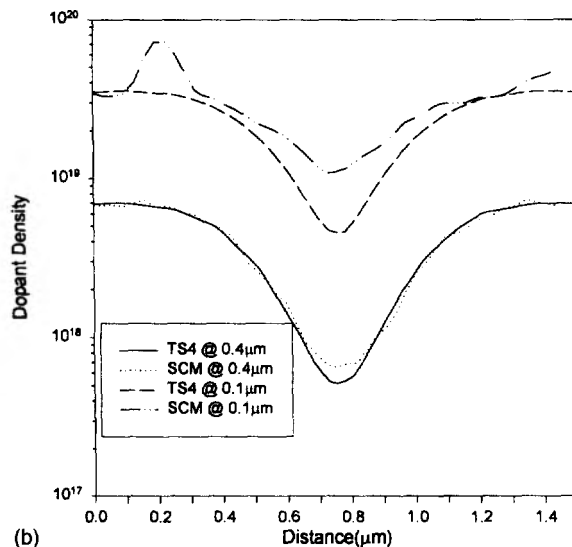
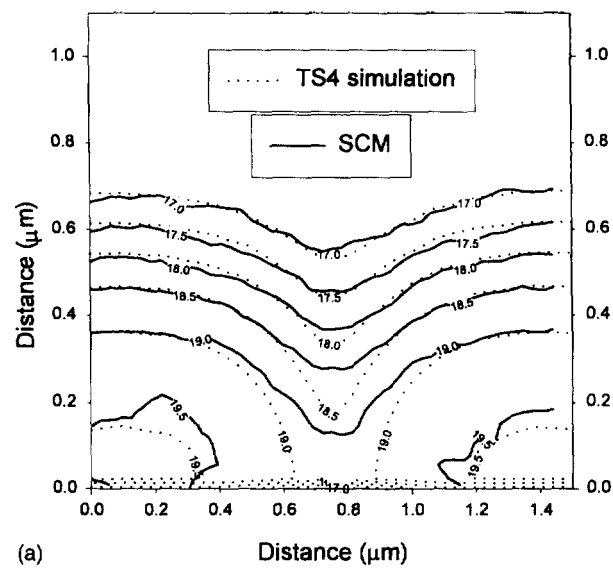


FIG. 4. (a) Contour plots of SCM and TSUPREM4 results on the diffused sample (sample 2). Numbers on the contour lines represent dopant concentration in $\log[\text{density}(\text{cm}^{-3})]$. (b) Lateral profile of the diffused sample at depths of 0.1 and 0.4 μm under the surface.

trend.¹⁴ Lateral junction positions must be controlled to less than 10 nm for current technology.¹ At issue, is the viability of 2D process diffusion to aid effectively in this quest.

IV. CONCLUSION

A two-step diffusion of dopants has been performed in two dimensions with SCM and TSUPREM4 process simulation. The process simulator has been tuned to best fit the SCM profile of the original sample both in vertical and lateral directions. This tuned simulator has been used for simulation of additional diffusion and compared with a SCM measurement on the diffused sample. Direct comparison of the 2D dopant profiles shows a moderate overall agreement. But underneath the gate, the process simulation underestimates the dopant density. However, we believe that our results should be an impetus and a basis for improved model parameter tuning in 2D simulators such as TSUPREM4.

ACKNOWLEDGMENTS

The authors would like to thank Digital Instruments, SEMATECH, and Semiconductor Research Corporation (SRC) for help and funding of this project and W. Wingert for sample preparation.

- ¹*The National Technology Roadmap for Semiconductors* (Semiconductor Industry Association, San Jose, CA, 1994).
- ²A. C. Diebold, M. R. Kump, J. J. Kopanski, and D. G. Seiler, *J. Vac. Sci. Technol. B* **14**, 196 (1996).
- ³Y. Huang, C. C. Williams, and J. Slinkman, *Appl. Phys. Lett.* **66**, 344 (1995).
- ⁴Y. Huang, C. C. Williams, and H. Smith, *J. Vac. Sci. Technol. B* **14**, 433 (1996).
- ⁵Y. Huang, C. C. Williams, and M. A. Wendman, *J. Vac. Sci. Technol. B* **14**, 1168 (1996).
- ⁶G. Neubauer, A. Erickson, and D. Adderton, *J. Vac. Sci. Technol. B* **14**, 426 (1996).
- ⁷J. S. McMurray, J. Kim, and C. C. Williams, *J. Vac. Sci. Technol. B* **15**, 1011 (1997).
- ⁸J. S. McMurray, J. Kim, C. C. Williams, and J. Slinkman, *J. Vac. Sci. Technol. B* **16**, 344 (1998).
- ⁹R. C. Palmer, E. J. Denlinger, and H. Kawamoto, *RCA Rev.* **43**, 194 (1982).
- ¹⁰C. C. Williams, J. Slinkman, W. P. Hough, and H. K. Wickramasinghe, *Appl. Phys. Lett.* **55**, 1662 (1989).
- ¹¹J. J. Kopanski, J. F. Marchiando, and J. R. Lowney, *J. Vac. Sci. Technol. B* **14**, 242 (1996).
- ¹²K. L. Westra, A. W. Mitchell, and D. J. Thompson, *J. Appl. Phys.* **74**, 3608 (1993).
- ¹³*TSUPREM4 User's Manual* (Technology Modeling Associates, Palo Alto, CA, 1996).
- ¹⁴For more discussions on the difficulties of calibrating process simulators and practical approaches to overcoming the difficulties, see S. S. Yu, H. W. Kennel, M. D. Giles, and P. P. Packan, *Tech. Dig. Int. Electron Devices Meet.*, p. 509 (1988); Also G. Le Carval, P. Schleiblin, D. Poncet, and P. Rivakin, *Proceedings of the 1997 International Conference on Simulation of Semiconductor Processes and Devices*, Cambridge, MA, 1997, p. 177.